*Proceedings of ITC18, 2008*

# Effects of gas-fueling by Supersonic Molecular Beam Injection on plasma performance in Heliotron J

Tohru Mizuuchi, Shinji Kobayashi, Satoshi Yamamoto, Hiroyuki Okada, Kazunobu Nagasaki, Shinya Watanabe[a], Kiyofumi Mukai[a], Katsuyuki Hosaka[a], Yusuke Kowada[a], Shiori Mihara[a], Hyunyong Lee[a], Yu Takabatake[a], Shintaro Kishi, Yuji Nakamura[a], Kiyoshi Hanatani, Nobuhiro Nishino[b], Shigeru Konoshima, Katsumi Kondo[a] and Fumimichi Sano

*Institute of Advanced Energy, Kyoto University, Gokasho, Uji 611-0011, Japan*
*[a]Graduate School of Energy Science, Kyoto University, Gokasho, Uji, Japan*
*[b]Graduate School of Engineering, Hiroshima University, Higashi-Hiroshima, Japan*

A gas fueling by supersonic molecular beam injection (SMBI) is successfully applied to ECH/NBI plasma in Heliotron J. Although the optimization of this fueling method for the Heliotron J experiment is in progress, increase/decrease of electron temperature and its target density dependence are observed for ECH plasma. In a combination heating condition of ECH (~ 0.35 MW) and NBI (~ 0.6 MW), the stored energy reached ~ 4.5 kJ, which is about 50 % higher than the maximum one achieved so far under the conventional gas-puffing in Heliotron J. Two different types of propagation of perturbations in the radiation profile are also observed after the SMBI for ECH+NBI plasma.

Keywords: fueling control, supersonic molecular-beam injection, gas-puffing, transport, Heliotron J

## 1. Introduction

The selection of gas fueling method is one of the most important factors to obtain a high density and good performance plasma from two aspects; (1) the profile control of the core plasma density through the controlled penetration depth of neutral particles and (2) the reduction of neutral particles in the peripheral region. Although injection of ice pellets is well known as a technique to realize favorable fueling from these aspects and used in rather large devices, the system is complicated and it is not easy to make a pellet small enough for density control in medium or small sized devices. On the other hand, a supersonic molecular beam injection (SMBI) technique, which has been developed by L. Yao et al. [1, 2, 3], is an alternative method to obtain the deeper penetration of the neutral particles into the core plasma compared to the conventional gas-puffing. This technique is considered to be effective especially for a medium or small sized device.

The SMBI technique has been used also for plasma diagnostics such as a He-beam probe or gas-puff imaging techniques in some fusion devices [4, 5], where the amount of the injected neutrals can be suppressed as low as possible to prevent the target plasma from being perturbed. Recently high-pressure SMBI is examined as a fueling method for ECH/NBI plasmas in Heliotron J.

This paper reports the first SMBI fueling experiment in Heliotron J. Although the optimization of this fueling method for the Heliotron J experiment is in progress, in a combination heating condition of ECH and NBI, the stored energy of ~ 4.5 kJ was recorded, which is about 50 % higher than the maximum one achieved so far under the normal gas-puff fueling condition [6] in Heliotron J.

## 2. Experimental Set-up

The Heliotron J device is a medium sized helical-axis heliotron device ($\langle R_0 \rangle / \langle a_p \rangle$ = 1.2/0.17 m, $B_0 \leq 1.5$ T) with an L/M = 1/4 helical coil [7, 8]. Figure 1 schematically shows the arrangement of the heating system, major diagnostic equipments and a SMBI system. The initial plasma is produced by using the second harmonic X-mode ECH (70 GHz, < 0.45 MW, non-focusing Gaussian beam) launched from a top port. The hydrogen neutral ($H^0$) beam (< 30 keV, < 0.7 MW/beam-line) is injected for NBI plasmas using one or two tangential

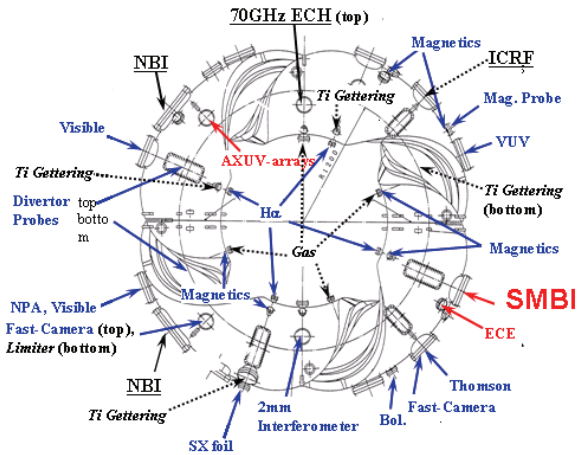


Fig. 1 Experimental set-up

*author's e-mail: mizuuchi@iae.kyoto-u.ac.jp*

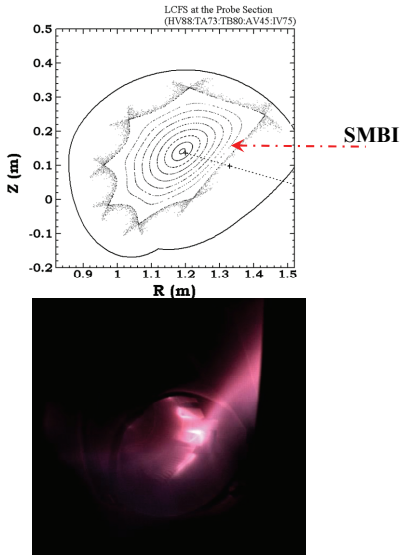


Fig. 2 The poloidal cross-section at the SMBI port (top) and a snapshot of the tangential plasma view (without any optical filter) at the timing of SMBI (bottom).

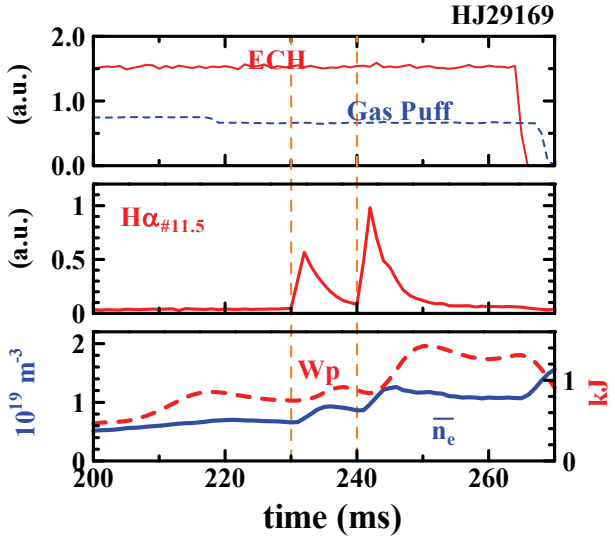


Fig. 3 Example of time traces of the intensity of Hα emission at the SMBI section, the line averaged density, the stored energy with ECH pulse and the gas-puff control voltage. The vertical dashed lines indicate the timing of SMBI.

beam-lines, which are facing each other (BL-1 and BL-2). Selecting one of the two beam-lines or changing the direction of the confinement field, Co- or CTR-injection can be performed.

A conventional gas-puff system with four piezoelectric valves is used to density control in usual experiments, which is installed at the inboard side ports around the torus at ≈90° intervals (see Fig. 1). In addition to this, a SMBI system is equipped on a horizontal port (#11.5 port) in Heliotron J. This system consists of a fast solenoid valve (the diameter of its orifice is 0.1 mm for this experiment.) with a magnetic shield. Although this system is introduced to Heliotron J originally for the diagnostic purpose such as the gas-puff imaging measurement for edge plasma turbulence with a high speed video camera [5], by increasing the plenum gas

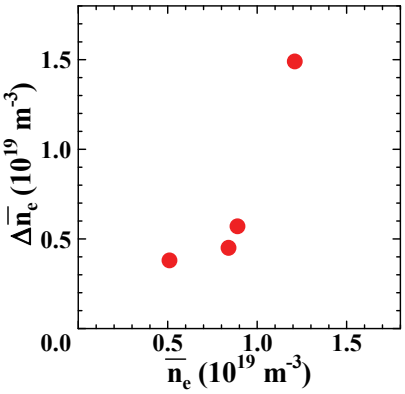


Fig. 4 The increase of $\bar{n}_e$ after a SMBI as a function of the target density (ECH plasma).

pressure (≥ 1 MPa) and the pulse width (0.4-1.0 ms), this system is used for the fueling control. Figure 2 shows a poloidal cross-section at the SMBI port and a snapshot of the tangential plasma view (with no optical filter) at the SMBI timing taken at the Thomson port near the SMBI port (see Fig. 1). By the SMBI fueling, a bright stripe is observed, which seems to be along the field line. Figure 3 shows an example of the time traces of the ECH pulse, the gas-puff control voltage, the intensity of Hα emission at the SMBI section ($H\alpha^{\#11.5}$), the line-averaged density ($\bar{n}_e$) and the stored energy ($W_p$) for an ECH plasma with SMBI, where the SMBI was fired two times with about 10 ms interval, indicated by the rapid increases of the Hα signal.

## 3. Experiments and results

### 3.1. SMBI for ECH plasma

The SMB pulse(s) of hydrogen was injected to ECH (~ 0.35 MW) deuterium plasmas of different line-averaged densities ($\bar{n}_e$) under the standard (STD) configuration [8] with the reversed magnetic field direction. Here, the condition of SMBI was fixed: the pulse width ~ 0.8 ms, the plenum pressure ~ 1.2 MPa. The experiment shows that the increase of $\bar{n}_e$ after a SMBI pulse ($\Delta\bar{n}_e$) seems to depend on the target density as shown in Fig. 4. Since the H-mode transition was observed above a critical density and $\bar{n}_e$ uncontrollably increases after the transition [9], it is difficult in higher $\bar{n}_e$ region to discriminate between the increase by SMBI itself and that due to the improved transport. The target density dependence of $\Delta\bar{n}_e$ observed in the low $\bar{n}_e$ region (< $1\times10^{19}$ $m^{-3}$), however, suggests the enhanced penetration of neutrals outside the plasma maybe due to the edge cooling by SMBI.

The difference in the $\bar{n}_e$ –$W_p$ relation between the conventional gas-puff and SMBI was not clear for ECH plasma with $\bar{n}_e$ well below the cut-off density. Near the cut-off density, however, the SMBI fueling seems better than the gas-puff from the viewpoint of the accessibility to the higher density and stored energy ECH plasma.

Figure 5 shows the time response of the ECE intensity $I_{ECE}$ from several channels, which corresponding to the different positions. Here the signals of Hα and $\bar{n}_e$ are also plotted. For higher target density plasma (~ $0.8\times10^{19}$

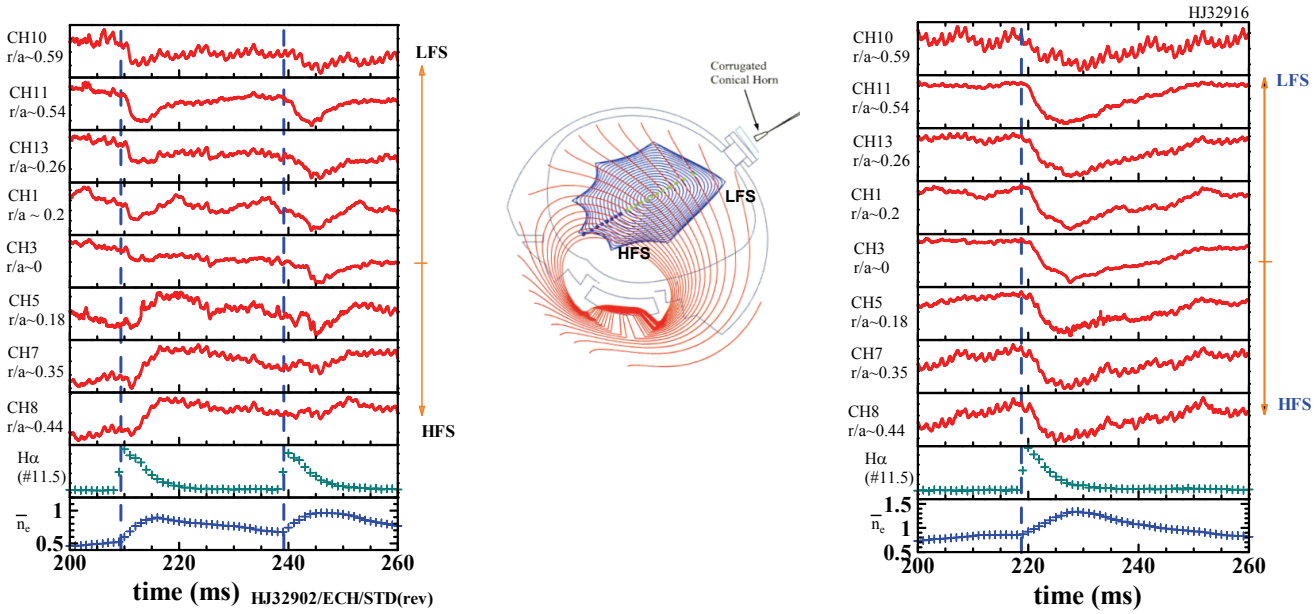


Fig. 5 Time responses of $I_{ECE}$ for a lower (left) and higher (right) target density plasma. (ECH plasma). The intensity of $I_{ECE}$ is adjusted to make clear the response for each channel. The middle figure schematically shows the poloidal section for the ECE measurement.

$m^{-3}$, Fig. 5 right), $I_{ECE}$ decreases after the SMBI pulse for all positions, indicating the decrease of electron temperature ($T_e$), and gradually recovers to the level before the SMBI. The start timing of the decrease in $I_{ECE}$ is almost the same for all channels, which might indicate some non-local phenomena. For lower target density plasma ($\sim 0.5\times10^{19}$ $m^{-3}$, Fig. 5 left), $I_{ECE}$ also decreases after the SMBI for the near side of the SMBI (i.e. the low field side, LFS). However, $I_{ECE}$ increases for the far side (i.e. the high field side, HFS), indicating the increase of $T_e$. Although we should take care of a local effect on $I_{ECE}$ since the ECE section is very close to the SMBI section, the increase of $T_e$ is interesting. The measurement of $T_e$ is necessary at a position toroidally well apart from the SMBI section. The measurement in more peripheral region is also necessary.

### 3.2. SMBI for ECH+NBI plasma

For the combination heating of ECH and NBI, the SMBI fueling is also preferable to produce higher $\overline{n_e}$ and higher $W_p$ plasmas. Figure 6 shows the time traces of $\overline{n_e}$, $W_p$, Hα and the signals from three channels of a SX-array for an ECH+NBI discharge with two pulses of SMBI. Here, the experiment was performed under the STD configuration with the normal field direction. The condition of ECH is almost the same as the experiment described in the previous sub-section and only one beam line (BL-2, ~0.6 MW) is used for NBI, i.e. the Co-injection. The first SMBI successfully increased the $\overline{n_e}$ and $W_p$, but the effect of the second SMBI was observed only on the slight increase of $\overline{n_e}$. The stored energy started to decrease before the second SMBI and was not increased by the second SMBI. Figure 7 shows the $\overline{n_e}$ dependence of $W_p$ for the similar ECH+NBI plasmas. Under the conventional gas-puff fueling, the stored energy are limited at ~ 3 kJ, By using the SMBI fueling, the stored

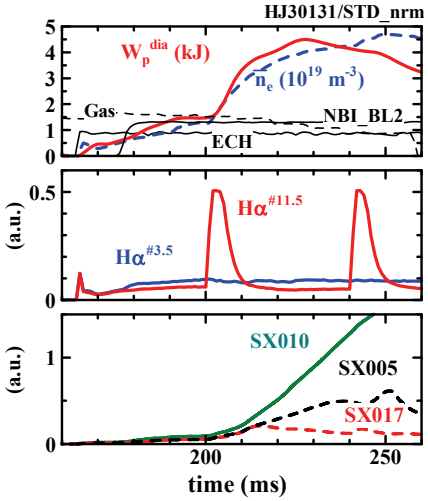


Fig. 6 Time traces of $\overline{n_e}$, $W_p$, Hα and $I_{SX}$ for an ECH+NBI discharge with SMBI.

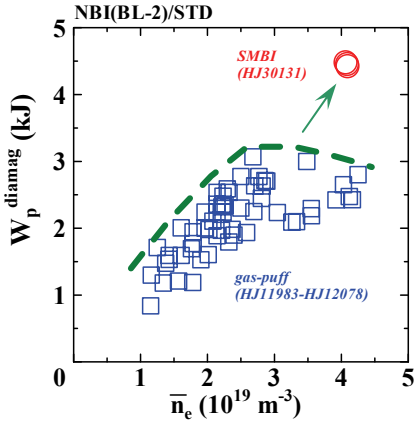


Fig. 7 The density dependence of the stored energy. (ECH+NBI plasma) □ are the data obtained with the gas-puff fueling and ○ are the data with the SMBI fueling.

energy reached ~4.5 kJ, about 50 % higher than the maximum value achieved under the conventional gas-puff fueling condition.

Relating to the SMBI effects on the plasma performance, propagation of perturbations caused by SMBI are observed in a chord-profile of radiation from the plasma measured with an AXUV-array. Here, the AXUV array with 1μm$^t$-Al filter was used for detection of radiation above ~500eV [10]. The discharge condition is a combination heating of ECH (~0.35 MW) and NBI (BL-1 and BL-2) under the STD configuration with the reversed field direction. Figure 8 shows the time responses of Hα, $\overline{n_e}$, $W_p$ and the normalized chord-profile of the radiation measured with the AXUV-array. As shown in the figure, we can observe two types of propagating perturbations in the radiation profile caused by a SMBI pulse; one is pinch-like perturbation near the center and the other is expansion observed in the peripheral region. Since the radiation is a function of the density and temperature, direct measurements of the temperature and density is necessary to understand this observation.

## 4. Summary

A gas fueling method with SMBI is successfully applied to ECH/NBI plasma in Heliotron J.

Interesting time responses caused by the SMBI are observed: increase/decrease of $T_e$ and its target density dependence for ECH plasma, two different types of propagation of perturbations in the radiation profile caused by the SMBI for ECH+NBI plasma.

In a combination heating condition of ECH and NBI, the stored energy reached ~4.5 kJ, which is about 50 % higher than the maximum one achieved so far under the conventional gas-puff fueling condition in Heliotron J.

In order to understand these interesting observations and to make use of these findings for improving plasma performance, more detailed studies and the refinement of the SMBI tourniquet are necessary. The optimization of this fueling technique for the Heliotron J experiment is in progress.

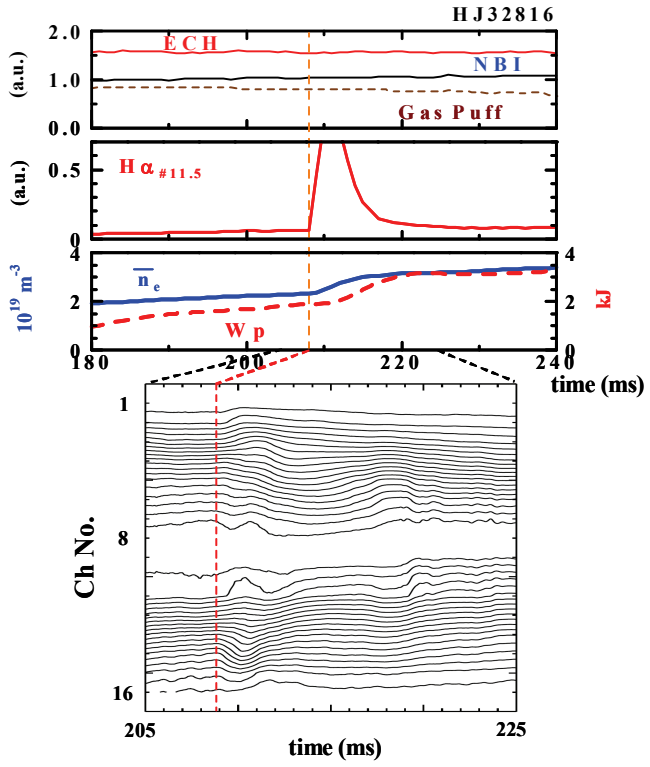


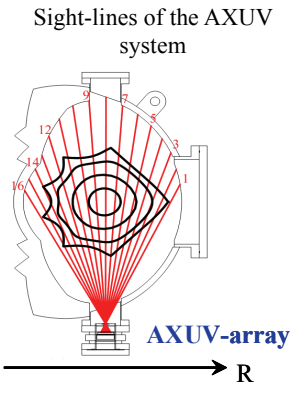


Fig. 8 Time responses of Hα, $\overline{n_e}$, $W_p$ and the normalized chord profile of radiation measured with the AXUV-array.

## Acknowledgement

The authors are grateful to the Heliotron J supporting group for their excellent arrangement of the experiments. The authors give special thanks to Profs. L. Yao, Q.W. Yang and their colleagues for the fruitful discussions. This work is performed with the support and under the auspices of the JSPS-CAS Core University Program, the Collaboration Program of the Laboratory for Complex Energy Processes, IAE, Kyoto University, the NIFS Collaborative Research Program (*NIFS04KUHL001, NIFS04KUHL002, NIFS04KUHL003, NIFS04KUHL004, NIFS04KUHL005, NIFS05KUHL007, NIFS06KUHL007, NIFS06KUHL009, NIFS06KUHL010, NIFS06KUHL011, NIFS06KUHL014, NIFS06KUHL015*) and the Formation of International Network for Scientific Collaborations as well as the Grant-in-Aid for Sci. Research.

References

[1] L. Yao, in "New Developments in Nuclear Fusion Research" (Nova Sci. Pub, 2006)) pp. 61-87.
[2] L. Yao et al., Proc. 20th EPS Conf. on Controlled Fusion and Plasma Phys. (Lisbon, 1993) vol. **17C(I)**, p303.
[3] L. Yao et al., Nucl. Fusion **47** (2007) 1399.
[4] B. Branas, et al., Rev. Sci. Instrum., **72** (2001) 602.
[5] N. Nishino, et al., J. Nucl. Mater., **337-339** (2005) 1073.
[6] T. Mizuuchi, et al., J. Plasma Fusion Res., **81** (2005) 949
[7] F. Sano, et al., J. Plasma Fusion Res. SERIES **3**, 26 (2000).
[8] T. Obiki, et al., Nucl. Fusion **41**, 833 (2001).
[9] F. Sano, et al., Nucl. Fusion **45**, 1557 (2005).
[10] S. Watanabe, et al., in this conference.